J. Biomed. Eng. Res : 30-37, 2006

Improved Current Source Design to Measure Induced Magnetic Flux Density Distributions in MREIT

Tong In Oh, Young Cho, Yeon Kyung Hwang, Suk Hoon Oh, Eung Je Woo, Soo Yeol Lee

Department of Biomedical Engineering, College of Electronics and Information, Kyung Hee University

(Received November 3, 2005. Accepted January 13, 2006)

Abstract

Injecting currents into an electrically conducting subject, we may measure the induced magnetic flux density distributions using an MRI scanner. The measured data are utilized to reconstruct cross-sectional images of internal conductivity and current density distributions in Magnetic Resonance Electrical Impedance Tomography (MREIT). Injection currents are usually provided in a form of mono-polar or bi-polar pulses synchronized with an MR pulse sequence. Given an MRI scanner performing the MR phase imaging to extract the induced magnetic flux density data, the current source becomes one of the key parts determining the signal-to-noise ratio (SNR) of the measured data. Since this SNR is crucial in determining the quality of reconstructed MREIT images, special care must be given in the design and implementation of the current source. This paper describes a current source design for MREIT with features including interleaved current injection, arbitrary current waveform, electrode switching to discharge any stored charge from previous current injections, optical isolation from an MR spectrometer and PC, precise current injection timing control synchronized with any MR pulse sequence, and versatile PC control program. The performance of the current source was verified using a 3T MRI scanner and saline phantoms.

Key words : MREIT, current source, magnetic flux density

I. INTRODUCTION

Cross-sectional imaging of electrical conductivity and current density distributions has been pursued in Magnetic Resonance Electrical Impedance Tomography (MREIT) [1-9]. When we inject current into an electrically conducting subject such as the human body through surface electrodes, there occurs a distribution of internal current density. Unknown internal conductivity distribution of the subject affects the current density distribution. Following the Biot-Savart law, the current density distribution produces a distribution of magnetic flux density. In MREIT, we obtain images of the magnetic flux density distribution using an MRI scanner to reconstruct cross-sectional conductivity and current density images.

Lately, it has been shown that MREIT imaging is possible by utilizing only one component of the induced magnetic flux density [10-15]. This technique is especially important since currently available MRI scanners can measure only one component of the magnetic flux density that is in the direction of the main magnetic field of the scanner. In this paper, we assume that this direction is parallel to the z-axis and the measurable component of the magnetic flux density is denoted as B_z.

In order to perform MREIT experiments, we should use a current source that injects current into the subject through surface electrodes. In most studies, currents have been injected as rectangular pulses synchronized with a chosen MR pulse sequence. Kim *et al.* developed a current source for a 3.0 T MREIT system [16] and it was used in experimental MREIT studies [17, 18]. From these studies, we found that the proper design and implementation of the current source is crucial to minimize the amount of artifact and noise in measured B_z.

Since the quality of the measured B_z images is the most fundamental factor to determine the quality of reconstructed MREIT images, special care must be given in the design and implementation of the current source. However, details of the MREIT current source design have not been reported yet. In this paper, we describe an MREIT current source with features including interleaved current injection, arbitrary current waveform setting, electrode switching to discharge any stored charge from previous current injections, optical isolation from an MR spectrometer and PC, precise current injection timing control

This work was supported by the SRC/ERC program of MOST/KOSEF (R11-2002-103) and the grant M60501000035-05A0100-03510 of KOSEF.

Corresponding Author : Eung Je Woo
Department of Biomedical Engineering College of Electronics and Informations, Kyung Hee Univ. 1 Seochun, Giheung, Yongin, Gyeonggi, 446-701, Korea
Tel : 031-201-2538 / Fax : 031-201-2378
E-mail : ejwoo@khu.ac.kr

for typical MR pulse sequences, and versatile PC control program. The performance of the current source was verified using a 3T MRI scanner and saline phantoms.

II. METHODS

A. Basic Setup to Measure Induced Magnetic Flux Density Images

Fig. 1 shows a basic setup for obtaining B_z images in MREIT. A subject is placed inside an MRI scanner and surface electrodes (four of them, for example) are attached on the subject. The MRI scanner has a main magnetic field B_0 in the z-direction. Lead wires connect electrodes to the switching circuit inside the MREIT current source. The waveform generator (WG) provides voltage signals and the voltage-to-current converter (VCC) injects current between a chosen pair of electrodes. The injection current pulses are synchronized with an MR pulse sequence using a trigger signal from the MR spectrometer. The voltmeter (VM) measures a voltage difference between other pair of electrodes for the use in conductivity image reconstructions [4-6, 10-12]. A micro-controller communicates with a PC and controls all functions of the current source.

Between a chosen pair of electrodes, we inject two current pulses of I^+ and I^- synchronized with a standard MR pulse sequence as illustrated in Fig. 2. The application of the injection current during MR imaging induces a magnetic flux density B= (B_x, B_y, B_z). The magnetic flux density B produces inhomogeneity of the main magnetic field and it causes phase changes that are proportional to the values of B_z. The corresponding MRI signals can be expressed as

$$S^+(m, n) = \int\int_{-\infty}^{\infty} M(x, y) e^{j\delta(x, y)} e^{j\gamma B_z(x, y) T_c} \cdot e^{j(x m\Delta k_x + y n\Delta k_y)} dxdy \quad (1)$$

and

$$S^-(m, n) = \int\int_{-\infty}^{\infty} M(x, y) e^{j\delta(x, y)} e^{-j\gamma B_z(x, y) T_c} \cdot e^{j(x m\Delta k_x + y n\Delta k_y)} dxdy \quad (2)$$

Here, M is the transverse magnetization, δ any systematic phase

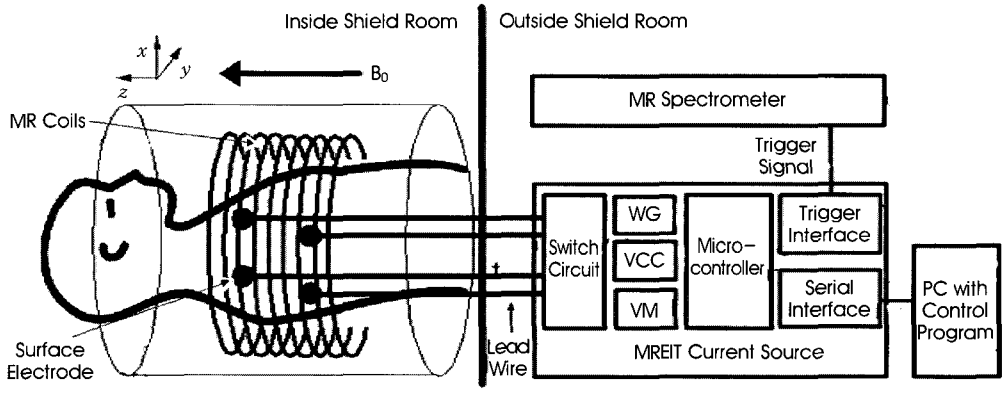

Fig. 1. Basic setup for obtaining magnetic flux density images in MREIT. The waveform generator (WG) outputs voltage signals and voltage-to-current converter (VCC) injects current between a chosen pair of electrodes. The injection current pulses are synchronized with an MR pulse sequence using a trigger signal from the MR spectrometer. The voltmeter (VM) measures a voltage difference between other pair of electrodes.

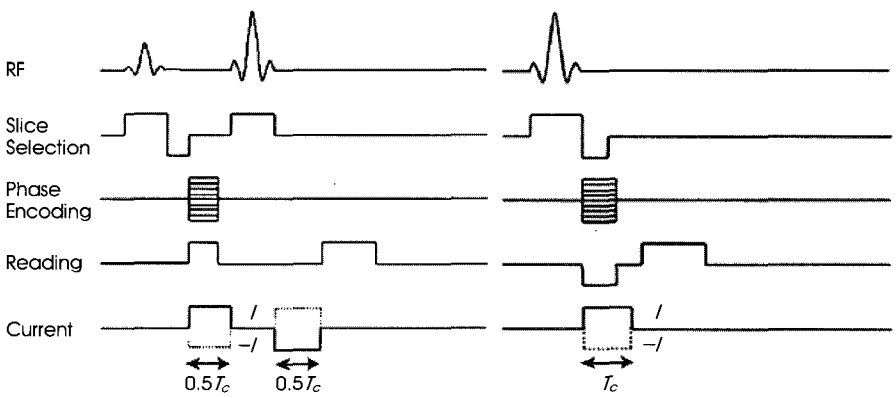

Fig. 2. Pulse sequences with synchronized injection current pulses. Current pulses with solid and dotted lines indicate I^+ and I^-, respectively. (a) Spin echo and (b) gradient echo.

error, $\gamma = 26.75\times10^7$ rad/T · s the gyromagnetic ratio of the hydrogen, and T_c the duration of current pulses as shown in Fig. 2.

Two-dimensional discrete Fourier transformations of S^+ and S^- result in two complex images of $\mathcal{M}^+$ and $\mathcal{M}^-$, respectively. Dividing the two complex images, we get

$$\mathrm{Arg}\left(\frac{\mathcal{M}^+(x,\ y)}{\mathcal{M}^-(x,\ y)}\right) = \mathrm{Arg}\left(e^{j2\gamma B_z(x,\ y)T_c}\right) = \Phi_z(x,\ y) \quad (3)$$

where $\mathrm{Arg}(\omega)$ is the principal value of the argument of the complex number ω. Since Φ_z is wrapped in $-\pi < \Phi_z \le \pi$, we must unwrap Φ_z to obtain ϕ_z. Finally, we get

$$B_z(x,\ y) = \frac{1}{2\gamma T_c}\phi_z(x,\ y) \quad (4)$$

B. Design Requirements

In designing an MREIT current source, we should consider factors affecting the quality of the measured magnetic flux density B_z. The quality can be evaluated in terms of random noise and systematic artifacts and we must minimize both of them.

The measured B_z data is contaminated with a Gaussian random noise from the MRI scanner. Based on the noise analysis by Scott *et al.* [19, 20] and also Sadleir *et al.* [21], the noise standard deviation s_B can be estimated as

$$s_B = \frac{1}{\sqrt{2}\gamma T_c \gamma_M} \quad (5)$$

where γ_M is the SNR of the MR magnitude image M in (1) or (2). With T_c=50 ms, we obtain $s_B = 2.02\times10^{-9}$ and 1.02×10^{-9} T when $\gamma_M = 50$ and 100, respectively. The SNR γ_M is primarily determined by the given MRI scanner and MR imaging parameters and little influenced by the current source. Therefore, in this paper, we assume that γ_M is pre-determined. The noise standard deviation s_B in (5) becomes the lower limit of the amount of random noise in measured B_z data. In order to attain this lower limit, the current source should not produce any additional random noise and systematic artifact.

First of all, we should be able to adjust the pulse width T_c so that we can properly set it for a given MR pulse sequence and imaging parameters. At the same time, the pulse width must be the same for both positive and negative current injection. This means that we should implement a precise timing control in the current source. The output of the current source must be noise-free in order not to generate any additional random noise in measured B_z images.

As shown in (1)-(4), we use both positive and negative injection currents to reject any systematic phase artifact δ and also to increase the phase change ϕ_z by the factor of two. This method works best when δ does not change with time and also the injection current pulses are identical except their polarity. Since there always exists some amount of drift in δ, we must minimize the time difference between positive and negative current injections. In addition, the current source must have an excellent reproducibility in terms of pulse shape, amplitude, and width. There should be no uncontrolled dc offset at the output of the current source for a precise polarity control.

In MREIT, we are mostly interested in the SNR of the measured B_z and it is mainly determined by the amplitude of injection current, size of the subject, electrode configuration, and the noise level expressed in (5). Regarding the amount of injection currents, it should be lower than the level that can stimulate muscle or nerve tissues. Although the amount depends on several factors such as the size and shape of electrodes, anatomical structure, and type of tissues, it is desirable to conform to the safety guideline [22]. For experimental MREIT studies using saline or tissue phantoms and postmortem animals, however, we may want to inject a large amount of current for better SNR in measured B_z images. Therefore, it is desirable to design a current source that can inject currents with variable amplitude of 0.1 to about 50mA.

C. MREIT Current Source Design

Fig. 1 shows the structure of the developed MREIT current source. In this section, we describe the details of the design. We begin with a PC program with graphical user interface to first provide the overall view of the current source.

PC Program with Graphical User Interface

We developed a current source control program running in a PC with Windows operating system (Microsoft, USA) and it provides a graphical user interface to setup injection current pulses in terms of its waveform, amplitude, and timing. Fig. 3 shows a screen capture of the PC program. We first establish a serial communication channel (either RS-232 or USB) with the micro-controller (TMS320LF2407A, Texas Instruments, USA) inside the current source. Then, we choose either spin echo or gradient echo pulse sequence. After setting up imaging parameters such as *TE*, *TR*, *NEX*, T_c, and number of slices, we can select an injection current waveform. Currently, three waveforms of rectangular, trapezoidal, and sinusoidal pulses are available even though we can use an arbitrary waveform stored in a hard disk of the PC. Then, we set the amplitude of the injection current pulse and the number of dummy triggers from the spectrometer that will be ignored by the micro-controller. The program allows us to choose electrode pairs for current injections and voltage measurements through the switching circuit. With all parameters properly set, the current source waits for the first trigger signal from the spectrometer. Receiving trigger

pulses, it injects currents as commanded by the PC program. During MREIT experiments, the program displays and stores the injection current waveform and measured voltage data.

Waveform Generator (WG)

Since the output impedance of the voltage-to-current converter cannot be infinite, there may occur loading effects due to the unknown load impedance of the imaging subject. Using rectangular pulses, we may end up injecting currents in a distorted waveform with overshoot and ringing or undershoot. Since the shape and area of the injection current pulse must be reproducible, it is sometimes better to use smooth waveforms such as sinusoids or trapezoids. In order to easily change the injection current waveform, the waveform data is downloaded from the PC to the micro-controller together with other imaging para- meters. The micro-controller stores the waveform data in its RAM and send them to a 16-bit DAC (AD768, Analog Devices, USA) that outputs voltage signals of the chosen waveform. The shortest pulse width for all three waveforms is 40μs.

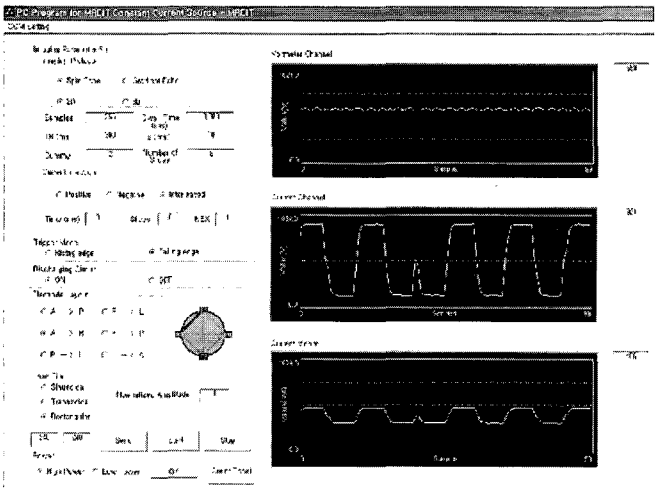

Fig. 3. Screen capture of the PC program that controls the MREIT current source.

Voltage-to-Current Converter (VCC)

The voltage signals from the waveform generator is converted to currents using the improved Howland current pump circuit [23]. In order to minimize the loading effect, the Howland circuit must have high output impedance. Therefore, we used a digital potentiometer (DS1267, Dallas Semiconductors, USA) to adjust the resistance ratio of the Howland circuit so that its output impedance becomes greater than 500KΩ at 100Hz. With the maximal current amplitude of ±45mA, the voltage-to-current converter based on an operational amplifier (OPA452TA, Texas Instruments, USA) has a voltage compliance of ±30V using ±35V dc power supply. The current amplitude can be adjusted in 256 steps from the maximal value. It is also possible to change the maximal current amplitude by manually setting an analog potentiometer inside the current source. We usually prepare two current sources with their maximal current amplitude values of ±45mA and ±5mA.

Switching Circuit

Using E number of electrodes, we can choose one of $E\times(E-1)/2$ number of electrode pairs to inject current. The switching circuit contains photo-MOS switches (AQY 212GS, Nais, Japan) with 0.34Ω ON resistance. These are controlled by the micro-controller to choose a pair of electrodes for current injection and other pair for differential voltage measurement.

Discharge Circuit

There exist capacitances between electrode-electrolyte interfaces. When we repeatedly inject current pulses with a non-zero dc value, charges may be accumulated in those capacitors. If we do not discharge them before injecting a subsequent current pulse, the stored charges may produce erroneous extra currents. In order to avoid this memory effect, we momentarily make the chosen pair of electrodes be short-circuited to the circuit ground after each current injection.

Trigger Pulse Interface

Trigger pulses from an MR spectrometer could be contaminated with switching and RF noise. In order to prevent the noise from entering the current source, the trigger pulse interface is based on an optical coupling device (ADUM1100BR, Analog Devices, USA). The minimum amplitude and width of a trigger pulse are 2V and 150ns, respectively. We can set the number of dummy triggers and then the micro-controller ignores those dummy triggers at the beginning of data acquisition.

Timing Control for Interleaved Current Injection

As described in the previous section, we inject positive and negative currents, I^+ and I^-, respectively. One of the primary reasons is to remove the systematic artifact δ in (1) and (2). Let us consider the pulse sequence in Fig. 4. First, we complete a data collection for S^+ with positive current pulses in (a). Then, we obtain S^- with negative current pulses in (b). In this case, the time difference between S^+ and S^- becomes longer. Since δ drifts during MR data collection period, there may remain some artifacts that are not cancelled out. To cancel out the systematic artifact as much as possible, the time difference between two sets of data S^+ and S^- must be minimal. For this reason, we use the interleaved current injection as shown in

Fig. 5. Here, we alternate injecting positive and negative current pulses for each horizontal scan line.

Voltmeter (VM)

In order to reconstruct images of a conductivity distribution in absolute values, we need to measure at least one boundary voltage induced by an injection current [4, 8, 11]. We can use a voltmeter that is based on an instrumental amplifier (AD620, Analog Devices, USA) to measure the voltage difference between a chosen pair of electrodes. We usually select a pair that is not being used for current injection. The measured voltage is digitized by the 10-bit ADC located inside the micro-controller (TMS320LF2407A, Texas Instruments, USA).

Power Supply and PC Interface

A separate isolated linear dc power supply providing analog ±35V and digital 5V is used for the entire circuits in the MREIT current source. The serial interface to exchange data with a PC is isolated using opto-couplers (HCPL9000, Agilent, USA) to minimize the digital noise coming from the PC.

D. Experimental Validation

To validate the performance of the MREIT current source, we used a cylindrical saline phantom of which design has been described in Oh *et al.* [17, 18]. The phantom was filled with a saline of 2S/m (12.5g/l NaCl and 2g/l $CuSO_4$) and we placed a hexahedral agar object of 0.5S/m (2g/l NaCl, 2g/l $CuSO_4$ and 15g/l agar) at the center. After placing the phantom with four recessed electrodes inside the MREIT system based on a 3T MRI scanner (Magnum, Medinus Inc., Korea) shown in Fig. 6(a), we obtained B_z images. We used the developed MREIT current source in Fig. 6(b) to inject currents into the phantom. The pulse sequence shown in Fig. 2(b) was used with the multi-slice gradient echo imaging technique. The amplitude of the injection current was 27mA with T_c=24ms. The number of slices was eight, the slice thickness was 3mm with no slice

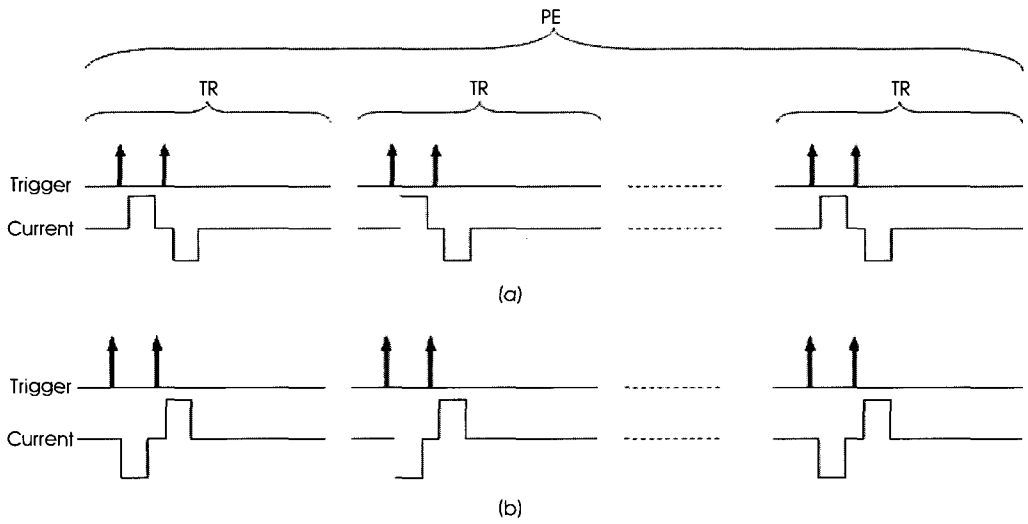

Fig. 4. MREIT injection current pulses synchronized with spin echo pulse sequence by trigger signals. (a) Positive current injection, I^+ and (b) negative injection, I^-.

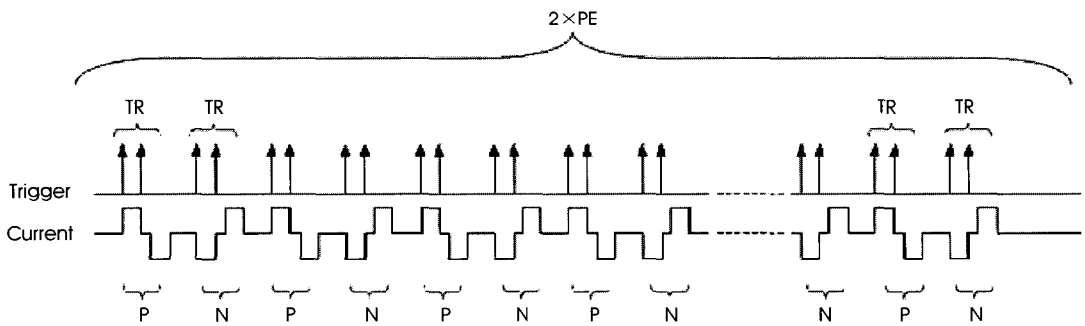

Fig. 5. Interleaved MREIT injection current pulses synchronized with spin echo pulse sequence by trigger signals. Positive I^+ and negative I^- current pulses are denoted as P and N, respectively.

gaps, *TR/TE* were 1400/60ms and *NEX* was 2. The image matrix size was 128×128 and field-of-view was 200×200mm^2 to result in a pixel size of 1.56×1.56mm^2.

III. RESULTS

Fig. 7 shows timing signals from the MR spectrometer measured by using a digital oscilloscope (TDS3014, Tektronix, USA). It also displays injection current pulses and switch control signals from the MREIT current source. We used a sinusoidal waveform in (a) and rectangular waveform in (b). Note that the rectangular pulse is distorted due to capacitive load of the saline phantom. In (a), the switch control signal is also shown and it connects current injection electrodes to the circuit ground to remove any stored charges. Comparing (a) and (b), it is clear that the smooth current pulse such as the sinusoid in (a) is advantageous since it allows us to inject current with the exact and predictable timing and shape. Fig. 8(a) and (b) show the signals with and without using the discharge circuit, respectively. As shown in (b) without using the discharge circuit, the envelope of several consecutive sinusoidal current pulses is not flat due to the memory effect.

Fig. 9 shows images of the saline phantom with injection current in the vertical direction. Fig. 9(a) is the MR magnitude image and (b) and (c) are measured phase and B_z image, respectively, at the middle imaging slice. Lately, Sadleir *et al.* [21] performed similar MREIT experiments using both 3 and 11T MRI scanners and the MREIT current source described in this paper. They found that the MREIT current source produces a negligible amount of systematic artefact in measured B_z images. The noise standard deviations evaluated from measured B_z images were close to the expected values in (5). Their results indicate that the MREIT current source described in this paper satisfies the requirements and it is possible to produce B_z images with a noise standard deviation of about 0.25nT at 3T field strength with the voxel size of 3×3×3mm^3 [21].

IV. DISCUSSION

In the developed MREIT current source, we tried to minimize the amounts of random noise and systematic artifacts. Precise timing control and high fidelity in injection current waveforms are essential to completely eliminate any systematic phase artifact δ in (1) or (2). These were achieved by the digital waveform gene- ration and accurate timing

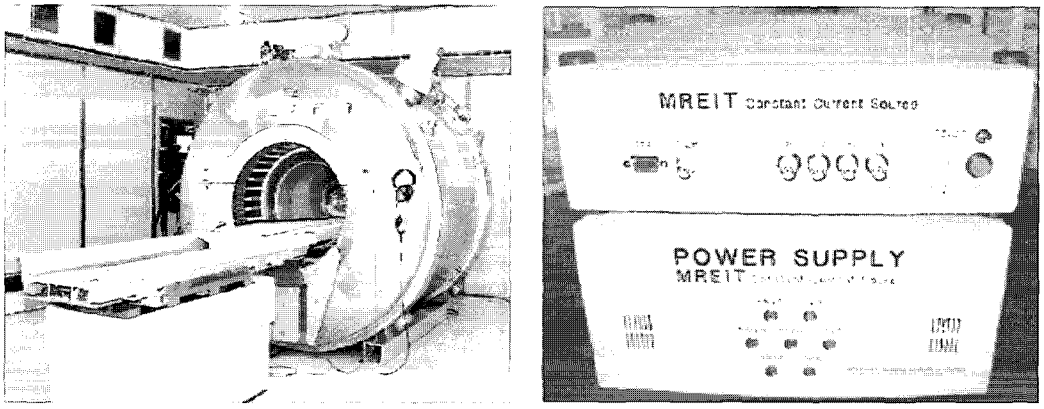

Fig. 6. (a) 3T MRI scanner and (b) MREIT current source.

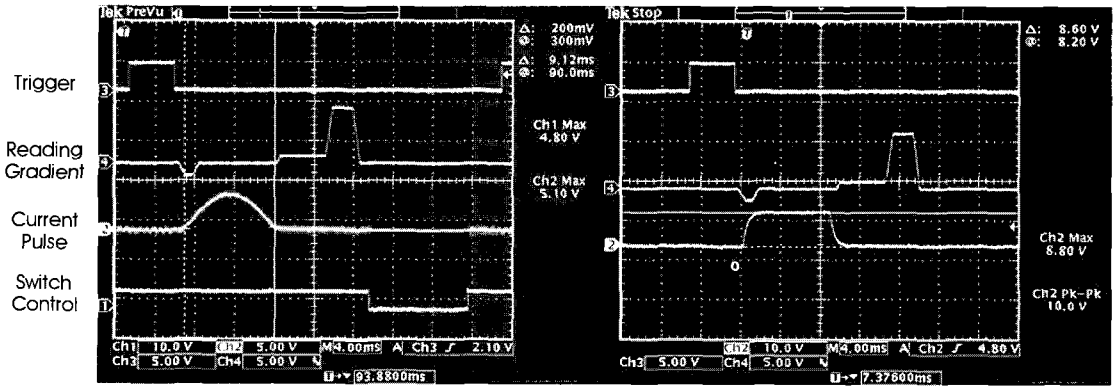

Fig. 7. Effects of a capacitive load for (a) sinusoidal and (b) rectangular current pulse. Signals were obtained with *TR*=300ms, *TE*=14ms, *I*=3mA and T_c=10ms.

control using a high-performance micro-controller. The interleaved current injection scheme was found to be very useful to significantly reduce the effect of any drift in δ.

The electronic noise from the developed MREIT current source was found to be negligible compared to the noise from the MRI scanner itself. This is due to the low-noise design including power supply, printed circuit board layout, optical isolations, and so on. In terms of the waveform, we found that trapezoidal waveform is desirable since it does not have steep edges and the area under the waveform could be larger than that of the sinusoid. We found that the switching circuit using photo-MOS switches are very useful. They not only simplify the experimental procedure of changing electrode pair but also enable us to use the discharge circuit to prevent any extra artifacts from occurring. In implementing any switching circuit, magnetic relays must be avoided since they may malfunction due to the fringe field of a high-field MR main magnet.

Like most constant current sources, the MREIT current source must have output impedance much bigger than load impedance. The output impedance was about 500KΩ at 100Hz. This value seems to be large enough not to produce any noticeable artifacts due to the resulting loading effect for most phantom and animal experiments [17, 18, 21]. However, in future works, it would be helpful to increase the output impedance beyond 500KΩ for human subjects with the skin.

For the lead wires, we used coaxial cables. Since the current source was located outside the shield room, we fed the cables through noise filters installed at the signal panel on the wall of the shield room. In order to reduce the cable length, it will be worth trying to put the current source inside the shield room. Future improvements should also include battery operation for further noise reduction and faster timing control for current injections with wider frequency range.

V. CONCLUSION

Carefully designed MREIT current source can mini- mize the amounts of artifact and noise in measured magnetic flux density images. Since the quality of the magnetic flux density image is crucial in reconstructing accurate conductivity and current density images, the current source is an important part of an MREIT system. The developed MREIT current source shows that interleaved current injection and appropriate electrode switching are quite useful to reduce systematic artifacts. Current source design with low-noise characteristics and high output impedance are needed to minimize the noise level in measured

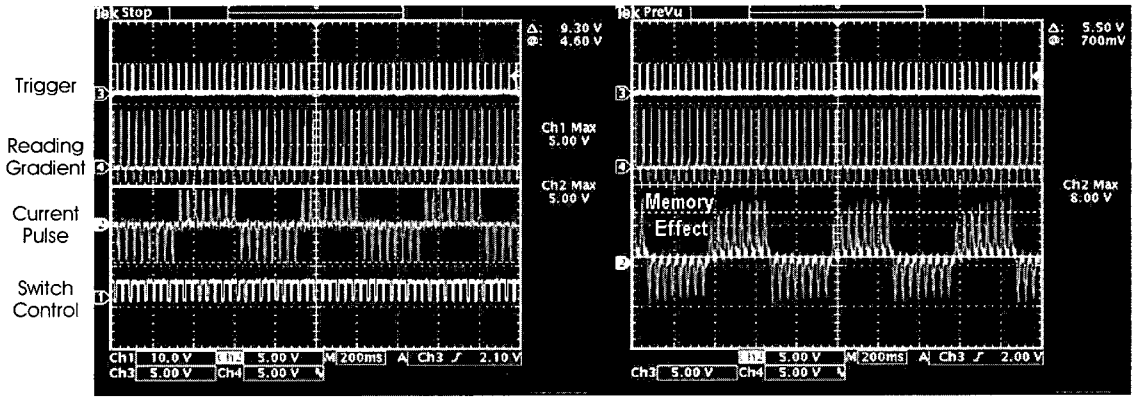

Fig. 8. Memory effect was not observed in (a) where the discharge circuit was used. Whereas, (b) shows the memory effect without using the discharge circuit. Signals were measured with the same condition as in Fig. 7.

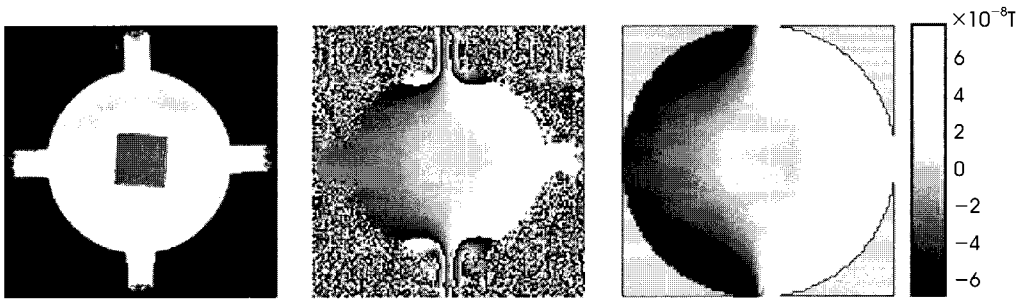

Fig. 9. (a) MR magnitude image of the saline phantom with an agar object at the center. (b) Phase image before phase unwrapping and (c) B_z image for the vertical current injection.

data. Future improvements should include the use of battery as dc power source. In addition, we should be careful in the way we place lead wires. Since we only measure the z-component of the induced magnetic flux density, it is better to run lead wires straight along the z-direction to avoid producing extra magnetic flux density in the z-direction due to the current along the lead wires. Currently, one of the most challenging technical problems in MREIT is to reduce the amount of the injection current. As we reduce the current, the induced magnetic flux density is consequently reduced. In order to keep the SNR high enough even with the reduced amount of injection current, future works should be focused on developing low-noise experimental and signal processing techniques.

REFERENCES

[1] N. Zhang, Electrical Impedance Tomography based on Current Density Imaging, MS Thesis, Dept. of Elec. Eng., Univ. of Toronto, Toronto, Canada, 1992.

[2] E. J. Woo, S. Y. Lee, and C. W. Mun, "*Impedance tomography using internal current density distribution measured by nuclear magnetic resonance*", SPIE, Vol. 2299, pp.377-385, 1994.

[3] Y. Z. Ider and O. Birgul, "*Use of the magnetic field generated by the internal distribution of injected currents for Electrical Impedance Tomography (MR-EIT)*", Elektrik, Vol. 6, pp.215-225, 1998.

[4] O. Kwon, E. J. Woo, J. R. Yoon, and J. K. Seo, "*Magnetic resonance electrical impedance tomography (MREIT): simulation study of J-substitution algorithm*", IEEE Trans. Biomed. Eng., Vol. 48, pp.160-167, 2002.

[5] H. S. Khang, B. I. Lee, S. H. Oh, E. J. Woo, S. Y. Lee, M. H. Cho, O. Kwon, J. R. Yoon, and J. K. Seo, "*J-substitution algorithm in magnetic resonance electrical impedance tomography (MREIT): phantom experiments for static resistivity images*", IEEE Trans. Med. Imag., Vol. 21, pp.695-702, 2002.

[6] O. Birgul, B. M. Eyuboglu, and Y. Z. Ider, "*Current constrained voltage scaled reconstruction (CCVSR) algorithm for MR-EIT and its performance with different probing current patterns*", Phys. Med. Biol., Vol. 48, pp. 653-671, 2003.

[7] B. I. Lee, S. H. Oh, E. J. Woo, S. Y. Lee, M. H. Cho, O. Kwon, J. K. Seo, and W. S. Baek, "*Static resistivity image of a cubic saline phantom in magnetic resonance electrical impedance tomography (MREIT)*", Physiol. Meas., Vol. 24, pp.579-589, 2003.

[8] Y. Z. Ider, S. Onart, and W. R. B. Lionheart, "*Uniqueness and reconstruction in magnetic resonance-electrical impedance tomography (MR-EIT)*," Physiol. Meas., Vol. 24, pp.591-604, 2003.

[9] M. L. Joy, "*MR current density and conductivity imaging: the state of the art*", *Proc. 26th Ann. Int. Conf.* IEEE EMBS, San Francisco, CA, USA, pp.5315-5319, 2004.

[10] J. K. Seo, J. R. Yoon, E. J. Woo, and O. Kwon, "*Reconstruction of conductivity and current density images using only one component of magnetic field measurements*", IEEE Trans. Biomed. Eng., Vol. 50, pp.1121-1124, 2003.

[11] S. H. Oh, B. I. Lee, E. J. Woo, S. Y. Lee, M. H. Cho, O. Kwon, and J. K. Seo, "*Conductivity and current density image reconstruction using harmonic B_z algorithm in magnetic resonance electrical impedance tomography*," Phys. Med. Biol., Vol. 48, pp.3101-3116, 2003.

[12] Y. Z. Ider and S. Onart, "*Algebraic reconstruction for 3D MR-EIT using one component of magnetic flux density*", Physiol. Meas., Vol. 25, pp.281-294, 2004.

[13] C. Park, E. J. Park, E. J. Woo, O. Kwon, and J. K. Seo, "*Static conductivity imaging using variational gradient B_z algorithm in magnetic resonance electrical impedance tomography*", Physiol. Meas., Vol. 25, pp.257-269, 2004.

[14] C. Park, O. Kwon, E. J. Woo, and J. K. Seo, "*Electrical conductivity imaging using gradient B_z decomposition algorithm in magnetic resonance electrical impedance tomography (MREIT)*", IEEE Trans. Med. Imag., Vol. 23, pp.388-394, 2004.

[15] O. Kwon, C. Park, E. J. Park, J. K. Seo, and E. J. Woo, "*Electrical conductivity imaging using a variational method in B_z-based MREIT*", Inv. Prob., Vol. 21, pp.969-980, 2005.

[16] K. S. Kim, T. I. Oh, S. M. Paek, S. H. Oh, E. J. Woo, S. Y. Lee, and J. Yi, "*Design and performance analysis of current source for 3.0T MREIT system*", J. Biomed. Eng. Res., Vol. 25, pp.165-169, 2004.

[17] S. H. Oh, B. I. Lee, T. S. Park, S. Y. Lee, E. J. Woo, M. H. Cho, O. Kwon, and J. K. Seo, "*Magnetic resonance electrical impedance tomography at 3 Tesla field strength*", Mag. Reson. Med., Vol. 51, pp.1292-1296, 2004.

[18] S. H. Oh, B. I. Lee, E. J. Woo, S. Y. Lee, T. S. Kim, O. Kwon, and J. K. Seo, "*Electrical conductivity images of biological tissue phantoms in MREIT*", Physiol. Meas., Vol. 26, pp.S279-288, 2005.

[19] G. C. Scott, M. L. G. Joy, R. L. Armstrong, and R. M. Henkelman, "*Measurement of nonuniform current density by magnetic resonance*", *IEEE Trans. Med. Imag.*, Vol. 10, pp.362-374, 1991.

[20] G. C. Scott, M. L. G. Joy, R. L. Armstrong, and R. M. Hankelman, "*Sensitivity of magnetic resonance current density imaging*", J. of Magn. Reson., Vol. 97, pp.235-254, 1992.

[21] R. Sadleir, S. Grant, S. U. Zhang, B. I. Lee, H. C. Pyo, S. H. Oh, C. Park, E. J. Woo, S. Y. Lee, O. Kwon, and J. K. Seo, "*Noise analysis in MREIT at 3 and 11 Tesla field strength*", Physiol. Meas., Vol. 26, pp.875-884, 2005.

[22] J. P. Reilly, Applied Bioelectricity: From Electrical Stimulation To Electropathology, Springer-Verlag, NY, USA, 1998.

[23] S. Franco, Design with Operational Amplifiers and Analog Integrated Circuits, McGraw-Hill, NY, USA, 2002.